

## SCINTILLATOR'S OPTICAL PATH CONTRIBUTION TO SIGNAL RISE TIME OF SIPM DETECTORS

Cătălin Neacșu<sup>1,2</sup> and Căta-Danil Gheorghe<sup>3</sup>

*The rise time of a detector's signal is a critical parameter for timing performance. In order to determine the impact of a scintillator's size and shape over the output signal rise time, several scintillators of different sizes were back-lighted with light pulses injected at different angles, directly into the scintillator's body. The rise time of the output signals was measured and the results were compared with the values obtained for direct sensor illumination. Results showed that a larger sized crystal causes a longer output signal rise time and that crystal shape plays an important role in the rise time, i.e. conical crystals, which are optimized for fast timing applications, result in very short rise times when compared with cylindrical crystals of similar size. The excess rise time introduced by scintillators ranges from 1.38ns for the smallest conical crystal up to 3.36ns for the largest cylindrical crystal. Compared with the 16-18ns measured for  $\gamma$ -ray generated pulses, it indicates that the scintillator size is not the main contributor to the output signal rise time*

**Keywords:** rise time, Silicon Photomultiplier, LaBr<sub>3</sub>(Ce) scintillator

### 1. Introduction

Silicon Photo-Multipliers (SiPM) are the solid-state alternative to the Photo-multiplier tube (PMT) for photon detection, in applications where time and/or energy measurements are required and are becoming an attractive solution in terms of cost whenever PMTs are not suitable. SiPM's advantages over PMTs are presented in the literature, the main ones being their small size, mechanical strength, low voltage operation and magnetic field immunity.

---

<sup>1</sup>Physicist, Nuclear Physics Department, Horia Hulubei National Institute of Physics and Nuclear Engineering - IFIN-HH, R-077125 Bucharest, Romania, e-mail: catalin.neacsu@nipne.ro

<sup>2</sup>PhD Student, Physics Department, University POLITEHNICA of Bucharest, Bucharest, Romania

<sup>3</sup>Teacher, Physics Department, University POLITEHNICA of Bucharest, Bucharest, Romania

IFIN-HH developed  $\gamma$ -ray detectors based on large area SiPM arrays, coupled with  $\text{LaBr}_3(\text{Ce})$  crystal scintillators to be used for spectroscopy applications. Detector timing performance was analyzed, their 246.2(16)ps Coincidence Resolving Time (CRT) being close to the one obtained with PMTs 179.4(13)ps but slightly larger [1] [2].

Timing resolution characterization of the detectors is based on Constant Fraction Timing [6] [8] and its implementation is described in Ref. [1] and [2]. The resolution obtained with this method depends on the signal rise time i.e. the resolution is better when the rise time is shorter. However, resolution cannot be improved indefinitely due to jitter  $\sigma_t$  caused by noise  $\sigma_n$  [6] [8].

$$\sigma_t = \frac{\sigma_n}{\left. \frac{dV}{dt} \right|_{V_t}} \approx \frac{t_r}{S/N}, \quad (1)$$

For best timing resolution, it is recommended that the amplifier bandwidth and signal bandwidth to be equal or close to each other [6]. The relation between signal rise time  $t_r$  and its bandwidth  $f_u$  is given [6] as:

$$t_r = \frac{0.35}{f_u}, \quad (2)$$

Each component of the detection system has a contribution in the final rise time of the output signal,  $t_r$ :

$$t_r = t_{Sc} \oplus t_{Si} \oplus t_{Mx} \oplus t_{PA}, \quad (3)$$

- $t_{Sc}$  - the contribution of the scintillator
- $t_{Si}$  - the contribution of the individual SiPM cell
- $t_{Mx}$  - the contribution of the multiplexing network for large arrays
- $t_{PA}$  - the contribution of the pre-amplifier/front end electronics

The  $\oplus$  sign means that the contributions do not add algebraically but their contribution is the result of more complex mechanisms and as a result we should consider correlation factors and the chain architecture of the system (i.e. one system component's output is the input of the next component) in estimating each individual contribution. This paperwork does not intend to elaborate these mechanisms and will focus instead on measuring the overall contribution of photons' optical path through the body of the scintillator, independent of scintillation mechanism contribution, which both are part of  $t_{Sc}$ .

Characterization of the system's electronic components showed that intrinsic rise time can be as low as 2ns [2] while the rise time was 16ns for  $\gamma$ -ray generated pulses with the same electronic system coupled with a scintillator. The difference between intrinsic and complete system rise time values is large and an understanding of the contribution of each component in the system is needed in order to further improve timing performance of the detectors.

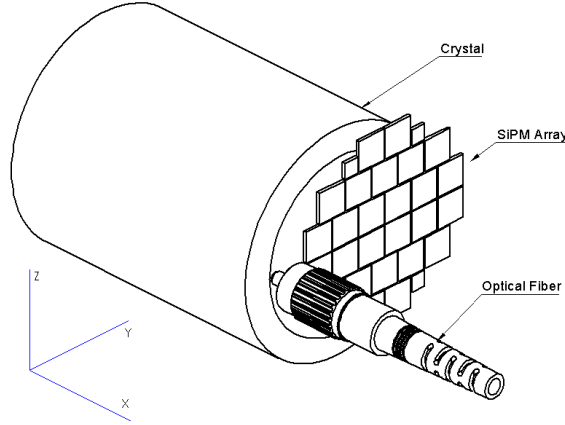


FIGURE 1. Experimental setup, 1.5" crystal shown

The goal of this work is to measure the contribution to the rise time of the scintillator's geometry and size while excluding the scintillation mechanism and at the same time keeping the rest of the system unchanged. In order to achieve the goal, we conducted an experiment in which light pulses were injected at different incident angles into the scintillator body and then we measured the rise time of the recorded pulses. As a reference we stimulated the SiPM array directly and measured the rise time of the output pulses.

Results shown that the scintillator size and geometry contributes with values in the range  $1.38 - 3.36ns$  to the output signal's rise time and concluded that it is not the main contributor to the rise time of the actual system.

## 2. Method

The arrangement of the experiment is shown in Fig. 1. The scintillator, optical fiber and SiPM array are held in place with the aid of 3D printed fixtures and the whole assembly is placed in a dark chamber. A CAEN SP5601 [14] system is used to inject light pulses in the scintillator at different incident angles ( $0^\circ$ ,  $30^\circ$ ,  $45^\circ$  and  $60^\circ$ ) by rotating the optical fiber around Z axis. The intensity of the light pulse is adjusted for each configuration to maintain the same peak value of the output pulse, in order to eliminate the variation of the rise time with pulse amplitude. The light exiting the crystal is collected by the coupled SiPM array, offset-ed in the +Y direction. Minimum 10000 events were recorded for each crystal-angle pair, using a Teledyne LeCroy HDO4104-MS at full bandwidth with the acquisition triggered by the output signal of SP5601. A Python [11] [9] [12] [10] script was used to compute the rise time of each pulse. The rise time values of a crystal-angle pair have a normal distribution as represented in Fig 5. All the measurements are centralized in Table 1.

In addition, the following measurements were taken:

- background radiation
- direct light pulse stimulation of the SiPM array at an incident angle of  $0^\circ$ .

### 3. Results and Discussion

The centralized results of the measurements for  $\text{LaBr}_3(\text{Ce})$  crystals are presented in Table 1 and Fig 2 & 3. Fig 5 shows the relative distribution of rise times measured for the 38x38 cylindrical crystal at  $0^\circ$  incident angle.

No.	$0^\circ$	$30^\circ$	$45^\circ$	$60^\circ$	D + L(inch)	Crystal
1	7.51(7)	7.23(6)	7.43(7)	7.66(7)	3.0	38x38 Cylindrical
2	7.95(8)	7.59(8)	7.83(8)	8.04(8)	3.5	38x51 Cylindrical
3	6.52(4)	6.32(4)	6.40(4)	6.38(4)	2.5	38x38 Conical
4	8.06(8)	8.04(9)	8.37(9)	8.32(9)	4.0	51x51 Cylindrical
5	8.3(2)	7.8(2)	7.9(2)	8.2(2)	6.0	76x76 Cylindrical

TABLE 1. Rise time (ns) for back lighted scintillators  
(D + L = diameter + length)

Although not documented by the crystal manufacturer, we can consider internal coating with a reflection coefficient close to 1 and both specular and diffuse reflection to exist at inner walls surface. In the following paragraphs, we will consider the front and the back faces the one in touch with the scintillator and its opposite respectively (along x axis per Fig. 1), and the distance between them, the length of the crystal while the other faces will be called sides. Based on this, we can explain the results as follows.

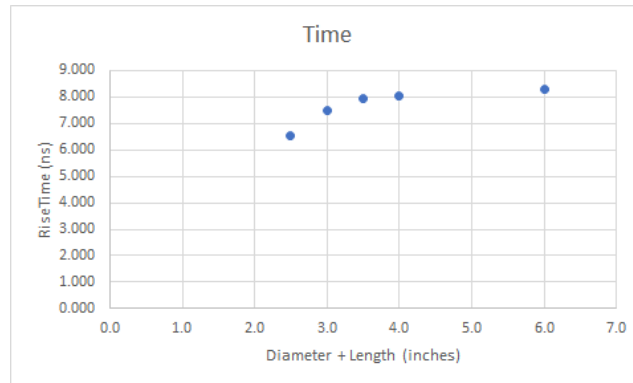


FIGURE 2. Rise time (ns) variation with linear dimension (half perimeter)

Fig. 2 shows the relation between the rise time and crystal linear dimension (Diameter + Length) for  $0^\circ$ . As expected, the rise time increases with linear dimension of the crystal, since photons need to travel a longer distance

between reflections before reaching the front face. However, as seen in this plot, rise time is not a linear function of the scintillator size. One of the main reasons for this is because in order to keep the electronic system unchanged, the same SiPM array was used for all the crystals and consequently the crystal area coverage by the SiPM array decreases with the increase in scintillator size. As a consequence, more photons are escaping the crystal without being detected by the SiPM thus the collection time is reduced, decreasing the contribution to signal rise time.

A notable result is obtained for the conical crystal which is significantly smaller than for the cylindrical ones of similar size. This result is explained by the angled side faces of the crystal, which causes the photons to reach the front face, thus the sensor, in a reduced number of reflections, reducing the travel time and thus improving the rise time. This is also confirmed by the small variation of the rise time with the incident angle of the light.

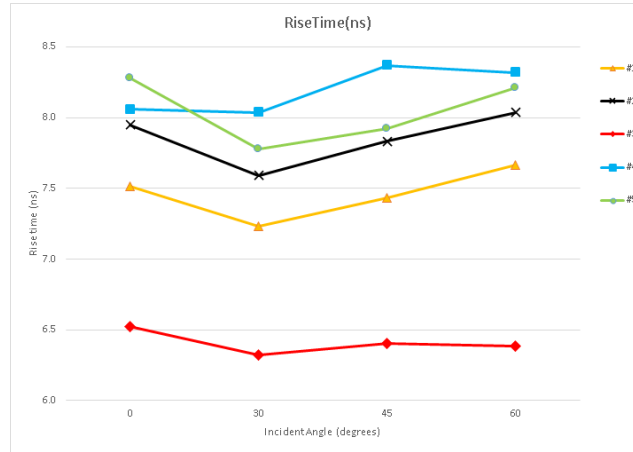


FIGURE 3. Rise time (ns) variation with incident angle plot legend numbers as in Table 1

At  $0^\circ$  incident angle, specular component of the reflection causes light to bounce back and forth between front and back faces of the crystal and the photons either exit the crystal through the uncoupled area of the scintillator or are absorbed by the walls after a large number of reflections. However, the diffuse reflection mechanism will still cause some photons to reach the SiPM array after each reflection but they will need more reflections to be directed to the sensor and a higher pulse intensity. The  $0^\circ$  values will be used as a reference in the next paragraphs.

At  $30^\circ$  incident, refraction angle is small and the light travels a distance close to  $2 \times L$  before reaching again the front face where it can be detected by the SiPM. The reflected photons will reach the SiPM area several times before reaching again an open area and escape the crystal. As a result, collection time is small and consequently rise time is shorter, as can be seen in Fig. 3

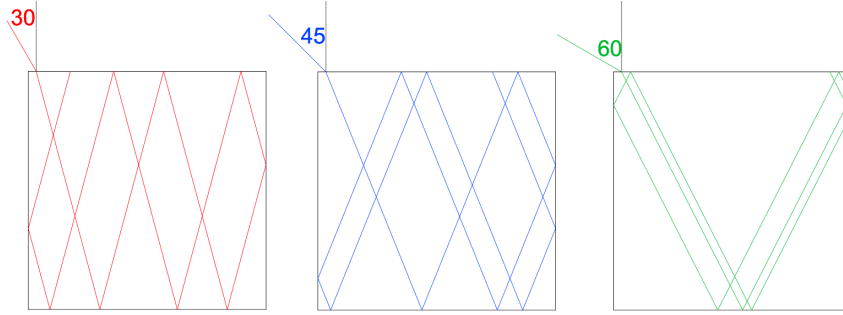


FIGURE 4. Specular reflections inside a crystal with  $L = D$  (simplified)

Further increasing the incident angle ( $45^\circ$  and  $60^\circ$ ) will cause the photons to travel longer distances between front and back faces of the crystal due to y-z speed component. They will behave like trapped light inside the crystal for a longer time as the angle is increased.

A notable result is curve #5, which corresponds to the 3 Inch crystal. All the measurements for angles  $> 0^\circ$  are smaller than the ones for #4 crystal. This is because, in order to keep the electronics system unchanged, the SiPM coverage area for the 3 Inch crystal is small. As a result, the probability of a photon to escape the crystal through the uncoupled area is very large (75%) and consequently it no longer contributes to the rise time. This way the measurements are "degraded" by this effect.

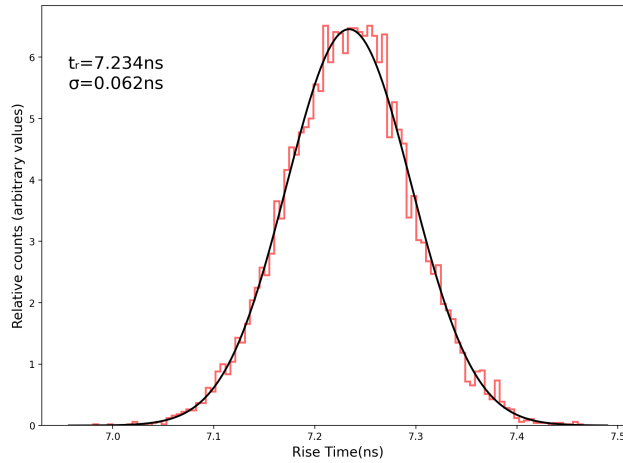


FIGURE 5. Rise time (ns) relative distribution, for the 38x38mm cylindrical scintillator and  $0^\circ$

Signal rise time of the sensor stimulated directly measured  $4.94(3)$  ns. This measurement provides a reference point and shows the lower limit of the experiment setup. Background radiation measurements are summarized in Table 2 and represent reference values for the complete detection system.

Scintillator	Rise time(ns)
LaBr <sub>3</sub> (Ce) 38x51mm	16.0(6)
LaBr <sub>3</sub> (Ce) 51x51mm	16.2(7)
LaBr <sub>3</sub> (Ce) 76x76mm	17.6(9)

TABLE 2. Rise time (ns) for background radiation

#### 4. Conclusions and Perspectives

The Array and FEE (Front End Electronics) used for this experiment are able to output pulses with a rise time as small as 4.94(3)ns when directly illuminated. When back-lighted, the rise time was between 6.32(4)ns and 8.32(9)ns. The rise time values for  $\gamma$ -ray generated pulses is in the range of 15-20ns (Table 2, Ref. [1],[2],&[3]).

We can conclude that the excess rise time introduced by the scintillators, due to optical path only, is small, in the range of a few ns (1.38-3.36ns as measured in this experiment) while one of the main contributors to the rise time difference between  $\gamma$ -ray pulses and back-lighted scintillators,  $\Delta t_r = t_r^\gamma - t_r^{bl} \in [8; 12]ns$ , is the scintillation mechanism.

The following aspects were not considered during the experiment and can be subject to further research.

The pulse width of CAEN SP5601 [14] is 8ns, being in the same range with the measurements in this experiment. Shorter pulses can be used in order to determine the rise time's lower limit of the Array and FEE and the impact in the final results. Papers [2] reported FEE rise time values as low as 2ns. In the end,  $\sigma_t$  (Eq. 1) is the parameter to be minimized for best timing performance.

Similar experiments may be conducted with PMTs in order to determine if the detector's interface material has any influence in the collection time of the photons. Trapping of light can occur due to different refractive indexes between scintillator and detector (PMT or SiPM) [7].

The fill factor of the SiPM array, which, due to manufacturing limitations, will always be less than 100%. Dead areas will influence resolution, rise time and dark count noise.

Other FEE design parameters can be analyzed [15] in order to further improve timing performance of SiPM large array detectors.

Monte Carlo simulations could be run, extending the work from Ref [4] & [5] to determine the impact of the optical path to the rise time.

#### REFERENCES

- [1] C. Mihai, G. Pascovici, G. Ciocan, C. Costache, V. Karayonchev, A. Lungu, N. Mărginean, R.E. Mihai, C. Neacșu, J.-M. Régis, A. Turturică, S. Ujeniuć and A. Vasiliu, Development of large area Silicon Photomultipliers arrays for  $\gamma$ -ray spectroscopy applications, Nuclear Instruments and Methods in Physics Research Section A: Accelerators, Spectrometers, Detectors and Associated Equipment, **953**(2020)

- [2] *G. Pascovici, C. Mihai, C. Neacșu, S. Ujeniuc, R. Mihai, C. Costache, N. Mărginean, A. Turturică, G. Ciocan, Jean-Marc Regis and V. Karayonchev*, The Use of Micro-Technologies in Nuclear Instruments, the Development of a Set of Modern Gamma-Ray Detectors Based on Sipm Arrays, *NANOMATERIALS – FUNCTIONAL PROPERTIES AND APPLICATIONS*, **28**(2020), 66-88, Editura Academiei Române
- [3] *J. Du, Y. Yang, X. Bai, M. S. Judenhofer, E. Berg, K. Di, S. Buckley, C. Jackson and S. R. Cherry*, Characterization of Large-Area SiPM Array for PET Applications, *IEEE Transactions on Nuclear Science*, **Vol 63**(2016), No 1, 8-16.
- [4] *Xin Yang*, Development of a Monte Carlo simulation tool for light transport inside scintillation crystals, Master of Science Thesis (2012)
- [5] *I. Mouhti, A. Elanique, M. Y. Messous, B. Belhorma, A. Benahmed*, Validation of a NaI(Tl) and LaBr<sub>3</sub>(Ce) detector's models via measurements and Monte Carlo simulations, *Journal of Radiation Research and Applied Sciences*, **Vol. 11, Issue 4, (OCT 2018)**, 335-339
- [6] *Helmuth Spieler*, *Semiconductor Detector Systems*, (2014), 179-188, Oxford University Press, United Kingdom
- [7] *Glenn F. Knoll*, *Radiation Detection and Measurement*, 4<sup>th</sup> Edition, (2010), 223-270, Wiley, USA
- [8] *William R. Leo*, *Techniques for Nuclear and Particle Physics Experiments: A How-to Approach*, 2<sup>nd</sup> Edition, (1994), 157-176, 325-334, Springer-Verlag, Germany
- [9] *Hunter, J. D.*, *Matplotlib: A 2D graphics environment*, *Computing in Science & Engineering*, Vol 9, 3(2007), 90-95, IEEE COMPUTER SOC
- [10] *Charles R. Harris, K. Jarrod Millman, St'efan J. van der Walt, Ralf Gommers, Pauli Virtanen, David Cournapeau, Eric Wieser, Julian Taylor, Sebastian Berg, Nathaniel J. Smith, Robert Kern, Matti Picus, Stephan Hoyer, Marten H. van Kerkwijk, Matthew Brett, Allan Haldane, Jaime Fern'andez del R'io, Mark Wiebe, Pearu Peterson, Pierre G'erard-Marchant, Kevin Sheppard, Tyler Reddy, Warren Weckesser, Hameer Abbasi, Christoph Gohlke, Travis E. Oliphant*, *Array programming with NumPy*, *Nature*, **Vol 585, 7825(2020)**, 357-362, Springer Science and Business Media LLC
- [11] *Pauli Virtanen, Ralf Gommers, Travis E. Oliphant, Matt Haberland, Tyler Reddy, David Cournapeau, Eugeni Burovski, Pearu Peterson, Warren Weckesser, Jonathan Bright, St'efan J. van der Walt, Matthew Brett, Joshua Wilson, K. Jarrod Millman, Nikolay Mayorov, Andrew R. J. Nelson, Eric Jones, Robert Kern, Eric Larson, C J Carey, İlhan Polat, Yu Feng, Eric W. Moore, Jake VanderPlas, Denis Laxalde, Josef Perktold, Robert Cimrman, Ian Henriksen, E. A. Quintero, Charles R. Harris, Anne M. Archibald, Antônio H. Ribeiro, Fabian Pedregosa, Paul van Mulbregt*, *SciPy 1.0: Fundamental Algorithms for Scientific Computing in Python*, *Nature Methods*, **17(2020)**, 261-272
- [12] *Raybaut, Pierre*, *Spyder-documentation*, Available online at: [python-hosted.org](http://python-hosted.org), (2009)
- [13] *ON Semiconductor*, *Silicon Photomultipliers (SiPM), High PDE and Timing Resolution Sensors in a TSV Package*, Rev. 6 Datasheet, (2018)
- [14] *CAEN*, *DS2447 - SP5601 Led Driver*, Rev. 3 Datasheet, (2014)
- [15] *Cătălin Neacșu et al*, *SiPM and readout equivalent circuits analysis in S-domain*, to be published (2021)